Contactless Charging and Communication System for Electric Vehicles

Albert Esser

Daimler-Benz AG
Goldsteinstr. 235
60528 Frankfurt
Germany

Abstract—Charging batteries in electric vehicles is the subject of several recent papers. These include electric safety, the weight of an on board charger, different types of chargers needed by different types of batteries, low line disturbance with high efficiency, and the influence of the charging process on the lifetime of the battery. Another important problem is the communication between the vehicle and the outside world during the charging process. This paper describes a system combining energy transfer and signal transmission in one unit, which is able to solve all of the above mentioned problems. Minimal power electronic components are installed in the vehicle. The system uses contactless energy transmission employing an inductive high frequency coupler. The charging process is monitored and controlled by an on board charge meter, which can communicate with the converter outside of the vehicle via the signal transmission included in the inductive coupler. A laboratory set-up able to transfer up to 5kW was build to demonstrate the performance of the system. The efficiency of the overall system including all filters, converters, and rectifiers is at a power level of 5kW better than 92%. The used gelled lead acid battery, 35Ah and 288V, was made from 24 battery modules.

1. The New Motivation to Run Electric Vehicles

Recently the interest on electric vehicles increases very much. Due to the new laws it is the first time that the environment for development and producing electric vehicles is stable. The renewed Clean-Air-Act of California forces the car makers to sale more than 2% of their cars in 1998 as zero emission cars and 2030 more than 10%. Therefore it makes sense economical to develop new electric vehicles.

All big american car makers (Chrysler, Ford, General Motors) developed prototypes of electric vehicles and working on salable cars today. The main task is to get the best operation behavior of the battery. On one side it is of interest to increase energy density of the battery /4/, on the other side to increase the lifetime. However, a battery monitoring system has to be installed and an optimal charging process has to be implemented to reach these goals /1/,/2/,/3/,/5/,/6/,/13/.

The activities in the field of battery research increased very much. Today no save decision can be made which kind of battery is the best for electric vehicles. In addition for different cars the energy storage capability has to be different. Due to these constrains a battery charger for electric vehicles has to be flexible.

1.1 The Contactless Charging System

To achieve a high lifetime of the battery, the battery charger and the charging process should adapted perfectly /1/. An On-Board charger can solve these problems, however the volume and weight of this charger is proportional to the charging power. For example the weight of a modern 3,5kW On-Board charger is about 15kg to 20kg (33lbs to 44lbs) /9/,/10/. An on board cord with a plug is used to connected the charger to a 230V household outlet. To achieve quick charging ability if the battery is completely discharged, results in a very high weight penalty.

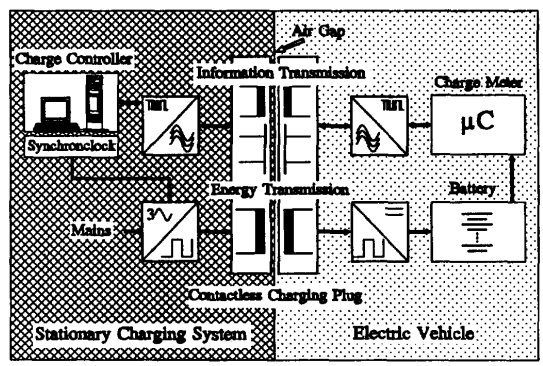

Figure 1: Structure of the Contactless Charging System

A charging system as shown in Figure 1 can be used to overcome the above mentioned problems. The contactless charging plug (CCP) is the key component in the system (Figure 1). It allows to transfer power and information in one compact unit. The energy is transferred inductively at a frequency of 25kHz. By variation of the turns ratio an adaption on the battery voltage can be achieved. To realize unity power factor and to get low line disturbances, the

0-7803-1462-x/93$03.00 ©1993IEEE

Authorized licensed use limited to: University of Maryland College Park. Downloaded on May 14,2026 at 21:43:15 UTC from IEEE Xplore. Restrictions apply.

IPR2026-00379
Tesla EX1018 Page 1

convert has to have sine wave input current.For information transmission the system provides two independent channels with a bandwidth of 1MHz each and a carrier frequency of 25MHz. They are used by the charge meter to transmit reference and measured values and to receive general information like amount of transferred energy and the price.

The charge meter is implemented as software on a PC-compatible microcontroller (V25). The information channels are used by the serial communication link (RS232) between the charge meter and the charge controller. The charge meter is sensing the battery current, temperature and module voltage. These are inputs of a Kalmann-Filter /2/ which calculates an estimation of the left charge and the lifetime of the battery. During charging the charge meter generates reference and measured values of the battery voltage and transmits them to the charge controller.

The charging process is controlled by the stationary charge controller. This structure allows to charge all kind of batteries in an optimum manner. Reference and measured value are generated by the charge meter. Only the current is controlled by the stationary part, because this dependents on the current capability of the converter.

2. Contactless Charging Plug (CCP)

This CCP (Figure 2) is basically an inductive coupler made from pot cores.

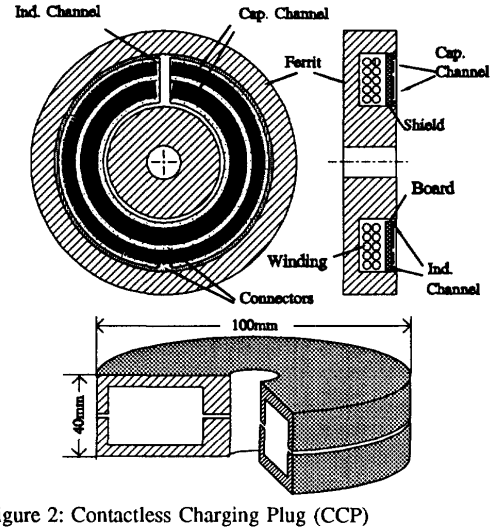

Figure 2: Contactless Charging Plug (CCP)

The contactless charging plug (CCP) shown in Figure 2 contains a ferrite potcore transformer and an integrated information transmission. One of the two halves belongs to the car, the other one to the stationary charging system. A similar system for robots is proposed in /14/,/15/,/16/,/17/.

The printed circuit boards placed near by the air gap provide signal transmission channels. The inductive channel as well as the capacitive channel is independent from the other and also from the field produced by the windings used for energy transmission. A data rate of up to 1MBit/sec is available in each channel besides the power transmission of several kW at the same time. This combined energy and signal coupler was introduced in /18/.

2.1 Inductive Energy Transmission

The inductive coupler for the energy transmission was made from the largest available potcore. The exact dimensions, including former and antennas, are shown in Figure 3. The recommended application for this potcore is the inductive switch. The ferrite material is N22 /19/, which is somehow similar to the material N27.

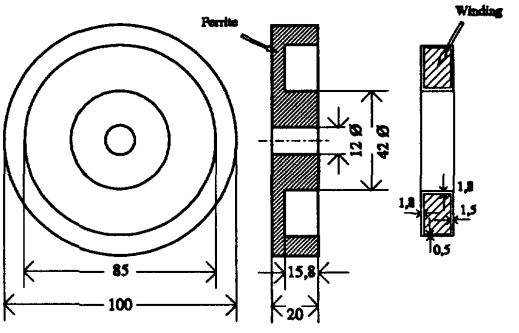

Figure 3: The Inductive Coupler

To investigate the influence of the air gap on the magnetic field, a finite element analyses was applied. The used software package was EMAS from McNeal/Schwendler.

The chosen air gap was 0.2mm. In Figure 4 a plot of the main field is shown; Figure 5 shows the leakage field. The length of the arrows is proportional to the value and the direction indicates the orientation of the magnetic field.

The disturbances in the main magnetic field caused (Figure 4) by the air gap is neglectable. However the field intensity is not constant over the magnetic path. Especially at the inner corner the value of the induction gets very high. This is caused by the geometry of this core. The cross section areas, where the flux has to go through, are extremely different. The cross section area at the inner corner is only 24% of the outer

Authorized licensed use limited to: University of Maryland College Park. Downloaded on May 14,2026 at 21:43:15 UTC from IEEE Xplore. Restrictions apply.

IPR2026-00379
Tesla EX1018 Page 2

air gap area. Also the inner air gap area is smaller than the outer one (58% of outer area).

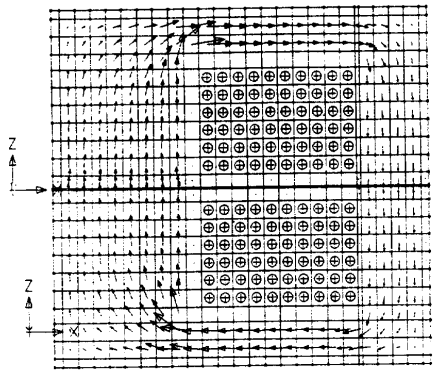

Figure 4: Plot of the Magnetizing Field, Air Gap 0,2mm

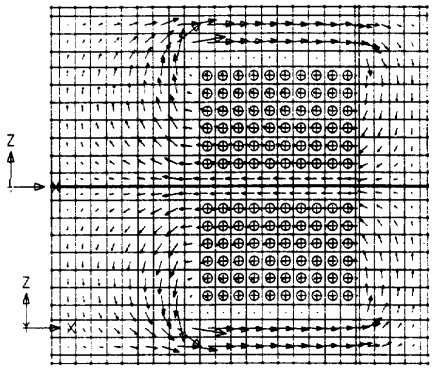

Figure 5: Plot of the Leakage Field, Air Gap 0,2mm

The leakage field (Figure 5) is like the main field not effected by the air gap. The leakage flux path goes through the ferrite. The intensity of the flux is effected by the geometry, as seen in the main flux.

The total flux through the core is the superposition of both. If the leakage and the main flux are not phase shifted, the total flux becomes higher than the magnetizing flux. The losses in the material are dependent of the highest value of the total flux. This is a principle disadvantage of this type of core. In /13/ a new type of transformer (coaxial wound transformer) is proposed, which overcomes this problem.

2.2 Information Transmission

Two different channels to transmit information are available. The inductive channel consists of a single turn winding (s. Figure 2) in each halve, which have no flux linkage with the main flux for power transmission. The windings have no common intersection with the flux leading air gap areas in the inductive coupler.

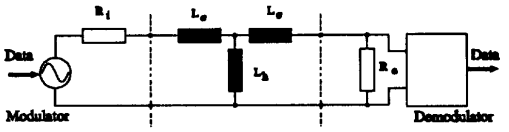

Figure 6: The Inductive Channel

The equivalent circuit of the inductive channel is shown in Figure 6. This channel is physically an air transformer inside the ferrite transformer. The coupling between these transformers is neglectable. The slot flux caused by the main field is practically zero (Figure 4). The leakage flux in the area of the air gap has a high value. However its direction is perpendicular to the winding area of the inductive antenna.

The capacitive channel is made by lamellated plates (Figure 2). The lamellation is necessary due to the field of the inductive channel to reduce damping, not due to the energy transmission. Assuming a very thin copper layer, there is no field to cause eddy currents in the capacitive antenna. To decouple the capacitive channel and the electric field of the winding for energy transfer, a shield is used. The shield can only cause common mode signals.

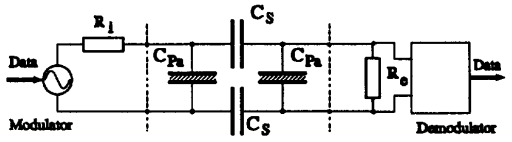

Figure 7: The Capacitive Channel

The capacitors C_S (Figure 7) can be used to transfer a differential mode signal to transmit information. The parasitic capacitors C_{Pa} are caused by the shield.

The measured transfer characteristics for both channels is shown in Figure 8. The channels both have band pass characteristic. At about 25MHz the channels have the lowest damping. Therefore the carrier frequency was chosen to 25MHz. The signal to noise ratio was measured with more than 20dB.

Authorized licensed use limited to: University of Maryland College Park. Downloaded on May 14,2026 at 21:43:15 UTC from IEEE Xplore. Restrictions apply.

IPR2026-00379
Tesla EX1018 Page 3

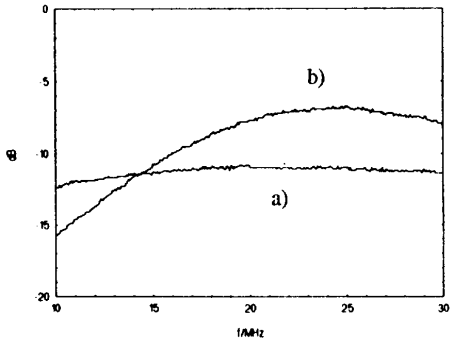

Figure 8: Plot of the Transfer Characteristics of
a) Inductive Channel
b) Capacitive Channel

3. The Converter

As energy source the three phase 230V, 60Hz system is chosen. In regard of the amount of electric vehicles and the needed energy a three phase connection is recommended. In /11/ a new three phase rectifier is proposed. With only one switch power factor improvement and reduction of harmonic distortion is possible. The basic principle is described in /12/ and named "Dither Signals."

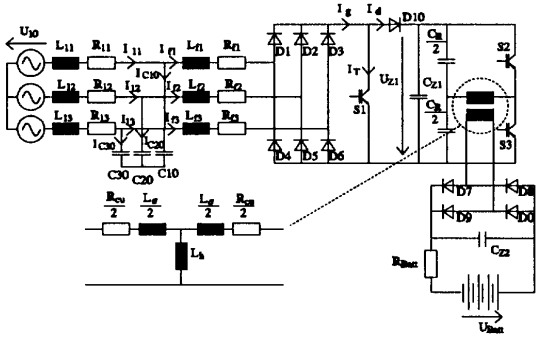

Figure 9: Converter Topology

The proposed converter topology for the contactless charging system is shown in Figure 9. A filter second order (L_{11}, R_{11} and C_{10}) is used to reduce the harmonic distortion. The boost choke usually placed on the DC side of the rectifier is distributed in the three phases (L_{f1}, R_{f1}). The boost converter is directly placed on the DC side of the rectifier. So fare the topology is identically with /11/.

A half bridge converter is connected on the DC link capacitor C_{Z1}. The capacitors $C_R/2$ are used to build a resonant circuit with the leakage inductance L_σ of the transformer. This allows to operate the converter with nearly no switching losses /14/. The secondary side of the transformer is part of the vehicle. The battery (U_{Batt}, R_{Batt}) is connected to another rectifier with a DC link capacitor C_{Z2}.

The whole system was analyzed by simulation. The relation between DC link voltage and total harmonic distortion (THD) was main point of interest.

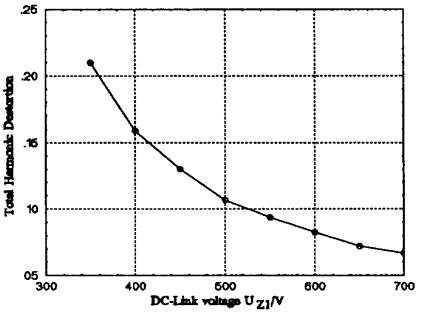

Figure 10: THD Analyses of the Line Current

The plot shown in Figure 10 is the optimal result to achieve. Therefore the current I_g has to be just on the margin between continues and discontinues mode. For example the line current wave form is shown in Figure 11 for to different levels of the DC link voltage U_{Z1}.

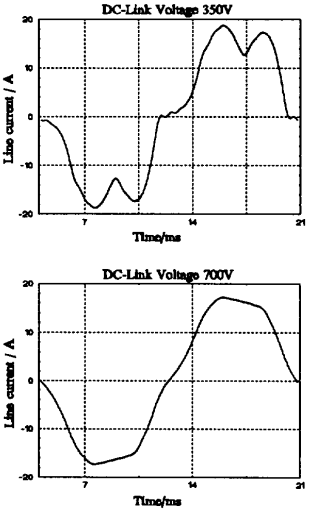

Figure 11: Line Current

Authorized licensed use limited to: University of Maryland College Park. Downloaded on May 14,2026 at 21:43:15 UTC from IEEE Xplore. Restrictions apply.

IPR2026-00379
Tesla EX1018 Page 4

The half bridge converter operates in resonant mode. The leakage inductance of the transformer (L_σ) is used with the capacitors C_R to build a series resonant circuit. The principle wave forms are shown in Figure 12.

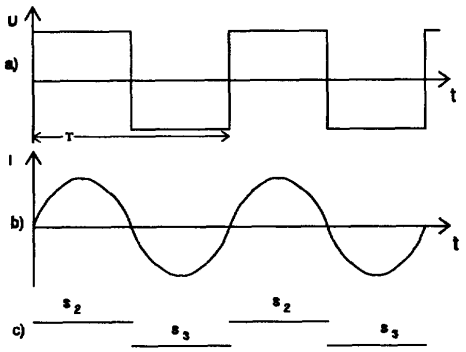

Figure 12: Principle Waveforms of
a) HF AC-Voltage,
b) Transformer Current,
c) Pulse Patterns

During switching, the current is very small. Only the magnetizing current is to switch.

The flux components in the transformer produced by this operation mode is shown in Figure 13. Leakage and magnetizing flux are phase shifted with 90°. For example, in Figure 13 the induction caused by the magnetizing flux is 200mT, the leakage induction is 20mT. As it is shown in Figure 13 the peak value of the total flux is never greater than the magnetizing flux. Since only the peak values are responsible for the amount of ferrite losses, the leakage field produces no additional losses in this operation mode.

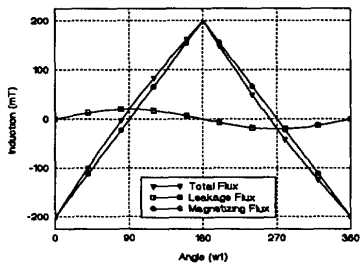

Figure 13: Induction Waveforms

4. Laboratory Set Up

The used battery was made from 24 modules. Each consists of six cells with a nominal voltage of 2V and a capacity of 35Ah (EXIDE). The lowest voltage, if the battery is completely discharged, is about 1.8V. The highest voltage during charging has to be lower than 2.35V.

Table 1
Data of the Laboratory Set Up

Filter-Choke	$L_{11}=L_{12}=L_{13}=1{,}316mH$	$R_{11}=R_{12}=R_{13}=54{,}7m\Omega$
Filter-Capacitors	$C_{10}=C_{20}=C_{20}=7{,}912\mu F$	$R_{f1}=R_{f2}=R_{f3}=121m\Omega$
Boost-Choke	$L_{f1}=L_{f1}=L_{f1}=102.867\mu H$	
DC-Link-Capacitor	$C_{Z1}=4000\mu F + 2\mu F$	
DC-Link-Capacitor	$C_{Z2}=1000\mu F + 1\mu F$	
Resonant-Capacitor	$C_R/2=500nF$	

The output voltage of the converter has to be in the range of 259.2V and 338.4V. As seen in Figure 10 the primary DC-Link voltage should be as high as possible. Therefore the turns ratio of the transformer was chosen 1:1, because the half bridge converter divides the output by factor 2. The converter components are listed in Table 1. This values are a result of the above mentioned simulation.

The switching frequency of the boost converter (switch S_1 and diode D_{10}) was chosen to 20kHz and of the half bridge to 25kHz. The line filter was designed with a natural frequency of 1.56kHz to damp the switching frequencies (>40dB) but not low order harmonics /7/,/8/.

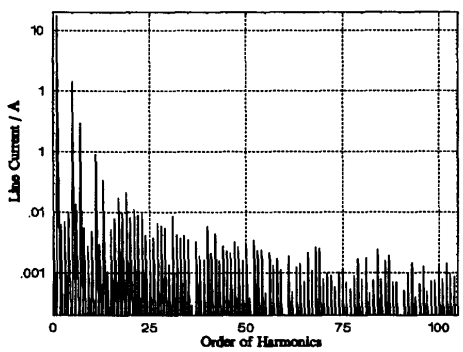

Figure 14: FFT-Analyses of the Line Current (U_{Z1}=650V)

A FFT-analyses of the system as a simulation result is shown in Figure 14. The 5^{th} and the 7^{th} harmonic are dominant. The THD is about 7.2%.

Authorized licensed use limited to: University of Maryland College Park. Downloaded on May 14,2026 at 21:43:15 UTC from IEEE Xplore. Restrictions apply.

IPR2026-00379
Tesla EX1018 Page 5

The transferable power through the transformer is 5kW at a temperature rise of about 40K.

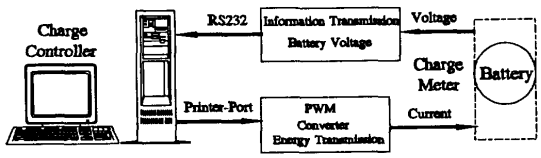

Figure 15: Data processing structure

The charge controller (Figure 1) is realized by a PC (Figure 15). The serial port (RS232) is used by the information transmission. The parallel port (printer port) is connected to a PWM controller which generates the pulse patterns for the boost switch and the half bridge.

4.1 Measurements

The above described set up was used to charge the battery repeatedly. In Figure 16 the plot of the battery current and battery voltage is shown. At the begin of charging the left charge in the battery was about 10% of the nominal capacity. Within the first seconds the current increases (Figure 16) until the power limit of the transformer is reached. After this a period of about 1500sec follows where the current is constant with 15A. The very slow decrease of the current within this period is caused by the constant power control. The battery voltage is increasing very slowly, so the current has to be reduced.

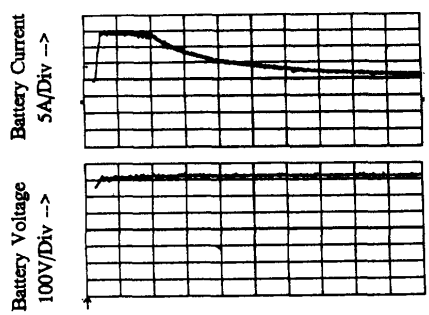

Figure 16: Battery Current and Voltage

If the battery voltage is 325V (this is less than the absolute maximum for safety) the voltage controller reduces the current.

The current and voltage of the energy transmission is shown in Figure 17. The transmitted power is 5kW. The current is sinusoidal and the voltage rectangular. During switching the current is very low and therefore the switching losses neglectable.

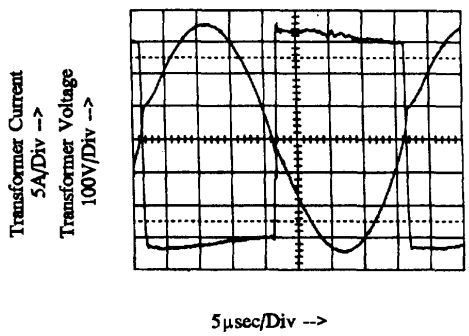

Figure 17: Transformer Current and Voltage (P=5kW)

In Table 2 the volume and weight is listed which is occupied by the car side power electronics. The needed weight is only 10% of the weight of a modern On Board charger.

Table 2
Volume and Weight of the Car Components

Weight of the CCP (one halve) including 0,5m wire	1,066kg
Weight of the rectifier at the battery including heat sink and wiring	0,502kg
Weight of the DC-link capacitor at the battery	0,39kg
Total weight of components to install at the electric vehicle	1,96kg
Total volume of the components to install at the electric vehicle	2Liter

The line current at 5kW charging power is plotted in Figure 18. The FFT-analyses of the line current is shown in Figure 19. The THD is 7.4%, which is very much the same as predicted by simulation (7.2%).

The efficiency of the whole system, including all filters, semiconductors and, transformer is shown in Figure 20.

Authorized licensed use limited to: University of Maryland College Park. Downloaded on May 14,2026 at 21:43:15 UTC from IEEE Xplore. Restrictions apply.

IPR2026-00379
Tesla EX1018 Page 6

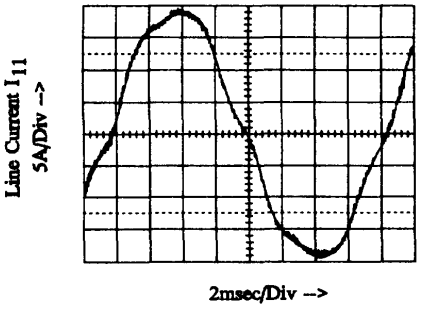

Figure 18: Line Current I_{11} (P=5kW)

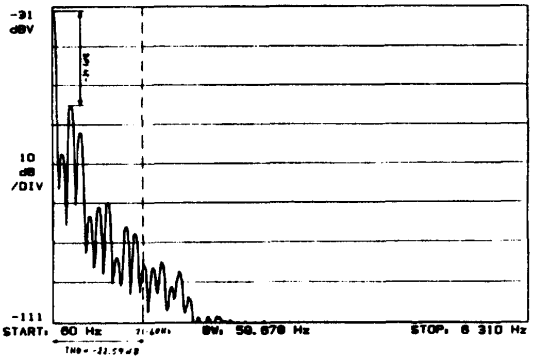

Figure 19: FFT-Analyses of the Line Current I_{11} (P=5kW)

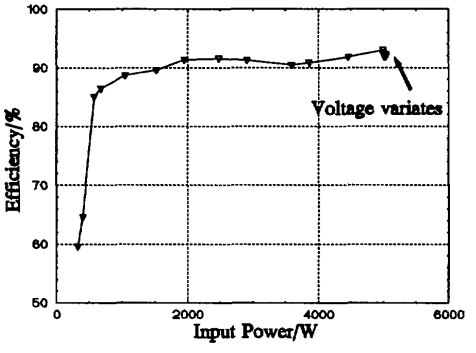

Figure 20: Efficiency of the Total System

5. Conclusion

A new system to charge batteries in electric vehicles is proposed. The contactless charging plug (CCP) is the key component of the system. Energy transmission and information transmission with one robust unit is possible by employing the CCP.

A three phase rectifier with power factor improvement and only one active switch is used to control the charging process and to reduce the THD of the line current.

A laboratory set up was build to verify the results of the simulation. Special features are the high efficiency (up to 93%) and the very low weight of the electric vehicle electronic components (2kg at 5kW).

The data processing is done by a PC, which is suitable for communication nets. This could be a link to the utilities to control peak power and rates. The information transmis-sion is used to transfer reference and measured values to a stationary charge controller. In addition a PIN code could be used to confirm a direct billing by the utility company.

Acknowledgment

This research project was funded by the "Deutsche Forschungsgemeinschaft (DFG)". The work was done at the Department of Electrical and Computer Engineering, University of Wisconsin, Madison, USA under supervision of Professor Divan. The author would like to thank the DFG for funding the project, Professor Deepak Divan and Professor H.-Ch. Skudelny for their generous support during this project.

References

/1/ W. Geuer, "Increasing Battery Life Time by Independent Cell Monitoring", 24th ISATA International Symposium on Automation, Florence, Italy 20-24th May 1991

/2/ H.P. Schöner, "Über die Auswertung des elektrischen Verhaltens von Bleibatterien beim Entladen und Laden", Dissertation RWTH Aachen, 1988

/3/ W. Steffens, "Verfahren zur Schätzung der inneren Größen von Starterbatterien", Dissertation RWTH Aachen, 1987

Authorized licensed use limited to: University of Maryland College Park. Downloaded on May 14,2026 at 21:43:15 UTC from IEEE Xplore. Restrictions apply.

IPR2026-00379
Tesla EX1018 Page 7

/4/ P. Lürkens, "Untersuchungen an leistungssteigernden Maßnahmen für den Bleiakkumulator", Dissertation RWTH Aachen 1989

/5/ J. Meiwes, "Untersuchungen zur Stromverteilung in Akkumulatoren", Dissertation RWTH Aachen 1986

/6/ D. Nowak, "Optimized Gas Controlled Charging of Lead Acid Batteries Using the Internal Battery Resistance as Charge Controller Feedback", EVS Nov. 13-16th 1988, Toronto, Canada

/7/ M. Albach, D. Dambois, "Optimized Operation Mode for 3 kW Off-Line Preconditioner Circuits", EPE Firenze, 1991, S. 134-139

/8/ M. Albach, "An AC-DC Converter with Low Mains Current Distortion and Minimized Conducted Emissions", EPE Aachen 1989, S. 457-460

/9/ J.Ch. Bendien, G. Fregien, J.D. v.Wyk, "High-Efficiency On-Board Battery Charger with Transformer Isolation, Sinusoidal Input Current and Maximum Power Factor", IEE Proc. Vol. 133, No. 4, July 1986, S. 197-204

/10/ J. Mućko, H.G. Langer, "A Noval Resonant DC to DC Converter with High Power Density and High Efficiency", EPE Aachen 1989, S. 1467-1471

/11/ A.R. Prasad, P.D. Ziogas, S. Manias, "An Active Power Factor Correction Technik for Three-Phase Diode Rectifiers", IEEE Transaction on Power Electronics, Vol. 6, No. 1, January 1991

/12/ I. Takahashi, "Power Factor Improvement of a Diode Rectifier Circuit by Dither Signals", IEEE / Industry Applications Society Annunal Meeting, 1990, S. 1289-1294.

/13/ K.W. Klontz, D.M. Divan, D.W. Novotny, R.D. Lorenz, "Contactless Battery charing System", United States Patent, Pat.-Nr. 5,157,319, Date of Pat. Oct.20,1992

/14/ A. Esser, Th. Kalker, "Berührungslose Energieversorgung dezentral angeordneter Antriebe in Handhabungsgeräten", etzArchiv, Bd. 12 (1990), H.8, S.259-264

/15/ A. Esser, H.-Ch. Skudelny, "A new approach to power supplies for robots", IEEE Transactions on Industry Applications, Vol. 27, Nr. 5, Sept./Okt. 1991, S. 872-875.

/16/ A. Esser, "Einrichtung zur kontaktlosen Übertragung von Wechselsignalen", Antrag auf Erteilung eines Patents, Aktenzeichen P 41 25 143.1, 1991

/17/ A. Esser, "Übertragungseinrichtung", Antrag auf Erteilung eines Patentes, Aktenzeichen P 41 25 143.8, 1991

/18/ A. Esser, "Berührungslose, kombinierte Energie- und Informationsübertragung für bewegliche Systeme", Dissertation RWTH Aachen 1992, Verlag der Augustinus-Buchhandlung Aachen, Germany, ISBN 3-86073-046-0

/19/ ———, "Ferrite und Zubehör", Datenbuch, Siemens Aktiengesellschaft

Authorized licensed use limited to: University of Maryland College Park. Downloaded on May 14,2026 at 21:43:15 UTC from IEEE Xplore. Restrictions apply.

IPR2026-00379
Tesla EX1018 Page 8